A Simplified Methodology for Remaining Life Prediction of Dents

Colin Scott, Mehrdad Palizi
AP Dynamics

Organized by

https://doi.org/10.52202/078572-0014

https://doi.org/10.52202/078572-0014

Abstract

Pipeline operators routinely carry out inline inspections to identify deformation on their pipelines, and specifically dents. Dents represent time-dependent failure mechanisms, as the flexing of a dent under pressure cycling conditions can result in crack initiation and fatigue growth. Recently developed dent assessment techniques have exposed various challenges to analysts, with industry finding difficulty in reaching consensus on an optimum methodology (Leis PPIM 2024).

In this work, we review the extensive published industry laboratory data. Various key parameters are investigated, including pipeline diameter and wall thickness, dent depth, pressure cycling magnitude and R-ratio, and restraint conditions. Numerical analyses are used to focus on the key parameters of interest to the remaining life assessments. More importantly, we also highlight the key parameters that do not appear to play a significant role in predictions.

The result of the project is a simplified dent remaining life assessment methodology that focuses on a single key parameter to the assessment. The less-relevant parameters are disregarded, as they bring a complexity to the assessment with no apparent benefit. Preliminary analysis suggests an improvement in model reliability and the possibility of improved program efficiency for operators.

Keyword: Engineering assessment, dent, fatigue, remaining life

Introduction

The oil and gas industry currently uses API 1183 [1] for the assessment and management of pipeline dents. The Recommended Practice was first published in 2020, after years of effort, largely sponsored by USDOT PHMSA and PRCI. It outlines several levels of assessments, from a simplistic Level Zero, to providing guidelines for a complex Level 3 FEA dent analysis. The higher-level assessments are rigorous in their details, often requiring analysts to complete specialized workshops to learn the nuances and intricacies of the various assessment types.

The API 1183 assessment methodologies have been publicly disputed by Leis (2024) [2] and others. Questionable assumptions and inconsistencies have been noted. The complexities of the methodologies are not conducive to clear understanding of the implicit assumptions and uncertainties.

This report describes an attempt to provide industry with a simpler, and more transparent, methodology for dent assessment. It is a work in progress. This report describes preliminary observations and developments, which are expected to evolve as more data becomes available. Its conclusions should be considered as stepping stones on industry evolving understanding of the field.

Literature Review

Several documents supporting the development of the API 1183 methodologies were reviewed in detail [3-8]. Data was compiled from three of these reports, specifically PHMSA (2012) Table A.1-1 3], PHMSA (2017) Table 11 [5] and PRCI (2019) Table 4.2 [7]. Gaps in the data were filled using assumptions consistent with the rest of the information provided.

https://doi.org/10.52202/078572-0014

The three available reports provided 103 data sets from full-scale dent fatigue tests. For each test, information is provided on diameter, thickness, grade, dent depth, indenter curvature, pressure cycling range, and total cycles to leak failure.

Some of the dent tests were non-standard "plain" dents. Several dents were corroded. Some had girth or long seam welds interacting. Some were created by non-spherical indenters, including axial short bars, transverse long bars, and angled long bars. This makes some comparisons challenging. All data sets were compiled into one table.

It is common for industry to express fatigue lives in terms of a Spectrum Severity Index "SSI". This allows pressure cycling spectra to be normalized to a single number. A common basis for the SSI calculations is 90 MPa stress and a Paris exponent of 3. All experimental fatigue lives reported were converted to these "equivalent" cycles to failure. This normalization may not be considered appropriate due to non-linearities associated with elastic-plastic behaviour of dent deformations, but it provides a starting point.

There were no "baseline" tests reported, that is, pipe sections with NO dents. As such, it is not possible to determine the relative damage associated with each dent. It was noted that all restrained dents survived at least 100,000 equivalent cycles. This suggests a natural limit higher than this value.

Methodology

Strain Analysis

Strain is considered by current methodologies as a key consideration in dent fatigue assessment [1, 9-11]. The strain imposed on a pipe by an indenter can be estimated based on the diameter and wall thickness of the pipe, and the curvature of the dent and /or indenter.

Based on the ASME B31.8 methodology:

$$\epsilon = \frac{t}{2} \cdot \left[\frac{2}{OD} + \frac{1}{\rho}\right]$$

where

ϵ	strain in the circumferential (hoop) direction
t	wall thickness
OD	pipe diameter
ρ	dent radius

This is a simplified two-dimension approach. Both API 1183 and ASME B31.8 consider the three-dimensional strain state and a Von Mises equivalent strain. Given that most cracks in dents are observed to initiate in the axial-radial plane of the pipe, the circumferential strain is expected to be the dominant strain component.

Note that the strain has two components. The first, based on the diameter, is the strain that flattens the pipe from its natural convex shape. The second, based on dent curvature, can be estimated from geometry ILI caliper profile analysis or is known from the indenter geometry in a lab scenario. It is the strain to form a concave dent shape, this analysis assumes a re-entrant dent.

https://doi.org/10.52202/078572-0014

The assumption from the strain analysis is that a sharp dent, from a small rock or excavator tool, or sharp lab indenter, is more likely to cause higher strain damage that will decrease the dent's fatigue life. However, this conclusion is not fully supported by the laboratory data. **Figure 1** is a plot of the curvature strain versus fatigue life, for the plain dent data. It does not appear the initial strain damage has a significant effect on the fatigue life of the dent. The corroded dent data did show a correlation, but this can be attributed to variation in wall thickness due to metal loss. The strain estimate is a variable for the unrestrained dents as re-rounding curvature could not be inferred with any accuracy.

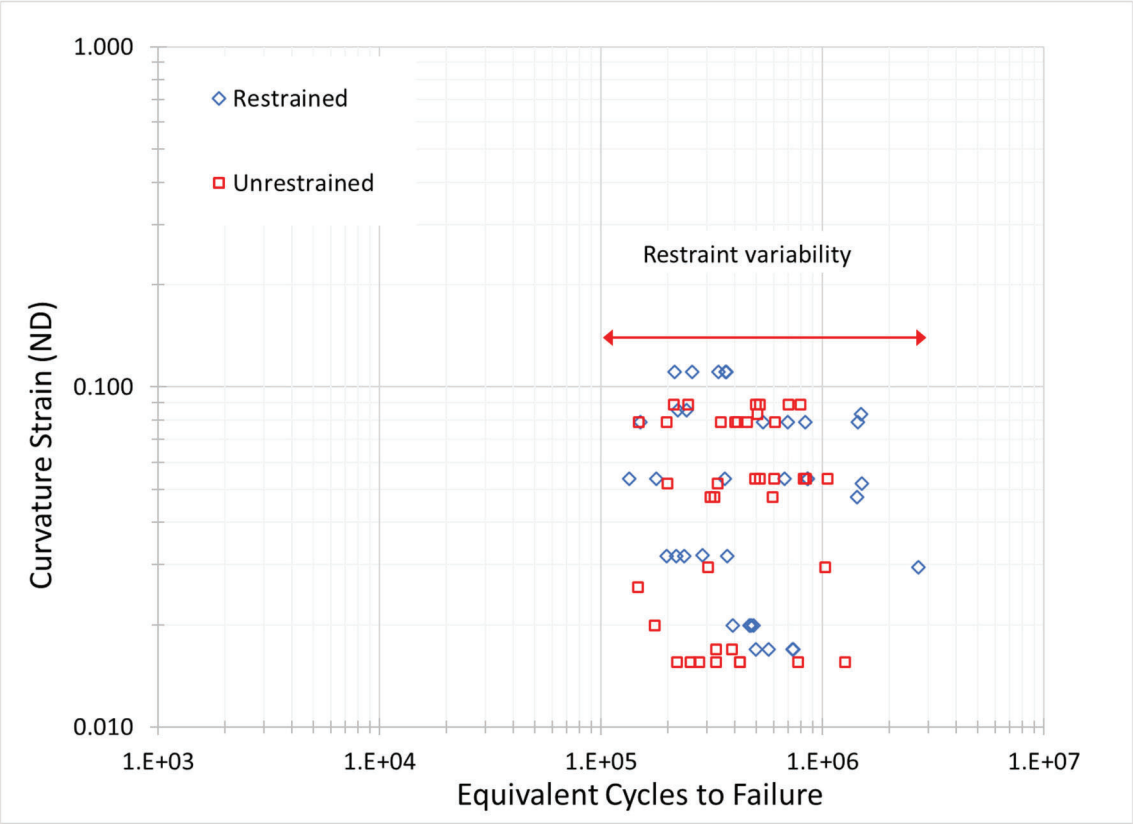

Figure 1 Plot of strain as a function of equivalent fatigue cycles to failure.

API 1183 Section 8.3.3.1 describes the "ductile fracture damage indicator" (DFDI) methodology for prediction of cracking during initial indentation. The PRCI (2022) [8] work reported various approaches to determining this strain value in preparation for forty-seven full scale tests. In the end "*in the 47 test results available, no cracks were observed during indentation*". The non-cracking result in all test cases, despite strain analysis predicting several critical strains, hints at the idea that this approach may be somewhat meaningless.

Based on the observation of minimal correlation between strain and fatigue life, it was decided to disregard the initial strain damage associated with the simplified dent assessment.

Stress Analysis

Stress is also considered by current methodologies as a key consideration in dent fatigue assessment [1, 9-11].

https://doi.org/10.52202/078572-0014

API 1183 methodologies often rely on "k" stress magnification factors. Many of these estimates are based on finite element analyses. The k-factors developed for API 1183 indicate higher values for deeper dents, higher (*OD/t*) ratios and /or restrained dents. The implication is that the higher stress magnification factors will decrease the dent's fatigue life. However, this is not necessarily consistent with laboratory studies, which indicate shorter fatigue lives for unrestrained dents. API 1183 Table 6 for Level Zero dent screening is based on the k-factors for the restrained dent analysis. This represents a logical inconsistency.

In this work, the stress is estimated from simple beam bending mechanics, rather than extensive finite element analysis. Two components are considered; the membrane stress associated with Barlow's formula (thin-walled pipe assumed) and the bending stress associated with pressure cycling on the internal faces of the dented pipe.

Pressure cycling at the pump stations is responsible for the stress cycling in the pipe walls. Using Barlow's equation:

$$\sigma_{mem} = P \cdot \left(\frac{D}{2 \cdot t_{nom}}\right)$$

Where

σ_{mem} membrane (hoop) stress in the pipe wall
P in-service pressure in the pipe
D pipe outside diameter
t_{nom} nominal wall thickness

This model development is based on the concept of "equivalent" cycles to failure, as described above. Assuming a standard 90 MPa equivalent stress,

$$\Delta P = 90 \cdot \left(\frac{2 \cdot t_{nom}}{D}\right)$$

Here we specify the nominal wall thickness as the basis for the pressure calculation. If the dent is corroded, we modify to account for the localized stress.

$$\Delta\sigma_{mem} \lesssim 90 \cdot \left(\frac{t_{nom}}{t_{loc}}\right)$$

where

t_{loc} local wall thickness due to corrosion

The locally decreased wall thickness serves to magnify the cyclic membrane stress in the dent wall. Note that the dent depth results in a slightly lower stress due to the shape change of the pipe cross section and less total pressure acting on the symmetry plane through the dent cross-section.

A typical fatigue assessment for an axial crack in a non-dented pipeline would focus on this hoop stress. The stress is primarily a membrane stress. In the case of a dent in a pipeline, a bending

https://doi.org/10.52202/078572-0014

component must be considered. This new proposed methodology focuses on estimating cyclic stresses from simple Euler beam bending equations. We will assume that the pipeline is in-service, the dent has re-rounded (or at least experienced a substantial service pressure to allow it) and elastic shake-down conditions apply.

The new methodology simplifies to the two-dimensional case. Consider the circumferential plane of the pipe cross-section, through the dent, see **Figure 2**. The width between the two shoulders is considered the dent "span".

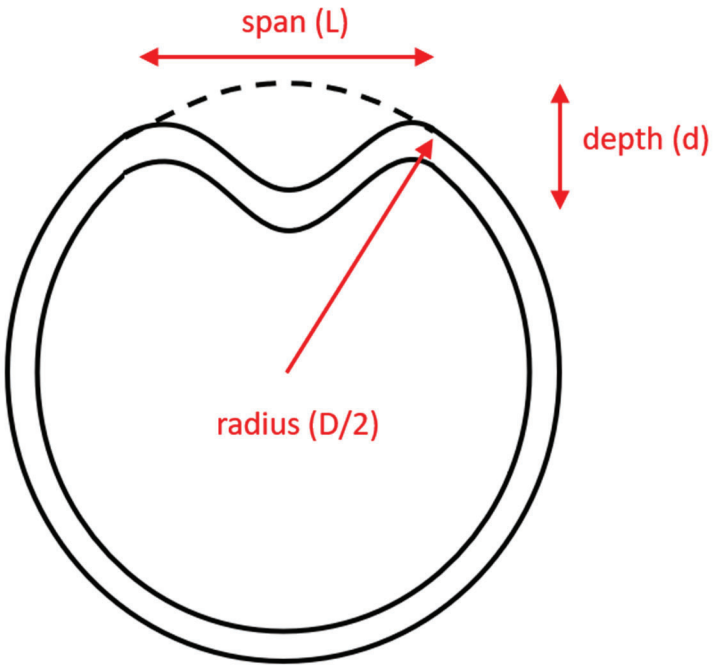

Figure 2 Schematic of pipe cross-section with dent for span length analysis.

We can now estimate the span as a function of the absolute dent depth. Using Pythagoras' Theorem and assuming $d << D$, we have:

$$\left(\frac{L}{2}\right)^2 = \left(\frac{D}{2}\right)^2 - \left(\frac{D}{2} - \frac{d}{2}\right)^2$$

and

$$L^2 \approx 2 \cdot D \cdot d$$

The moment acting in the span due to internal pressure can then be estimated by Eulerian beam mechanics [12]:

$$M = \frac{P \cdot L^2}{n}$$

where

M bending moment

https://doi.org/10.52202/078572-0014

L full dent span
n constraint factor

The constraint factor is determined by the conditions acting on the bending span. For a freely supported span, n = 8 at the centre of the span. For a restrained span, n = 12 at the fixed ends and n = 24 at the centre. Note that the total variation in the "n" constraint factor is 3x, suggesting a significant expected variation in stress conditions for conditions of partial restraint. A Paris Law exponent of 3 implies a (3^3 =) 27x variation in fatigue life. Recall that **Figure 1** indicated a variability in fatigue life of 30x, with no statistical effect of curvature strain.

The stress acting on the outer surface of the span is given by [12]:

$$\sigma = M \cdot \frac{c}{I} = M \cdot \frac{t_{loc}}{2} \cdot \frac{12}{{t_{loc}}^3} = M \cdot \frac{6}{{t_{loc}}^2}$$

At this point, we have not specified whether the dent is restrained or not.

Consider the case of the UNRESTRAINED dent, typically topside, see **Figure 3**. Cracking usually occurs on the outside surface, in the centre of the span where the curvature strain damage is the highest and the residual stress is tensile. The ends of the span are illustrated with red dot "hinge points".

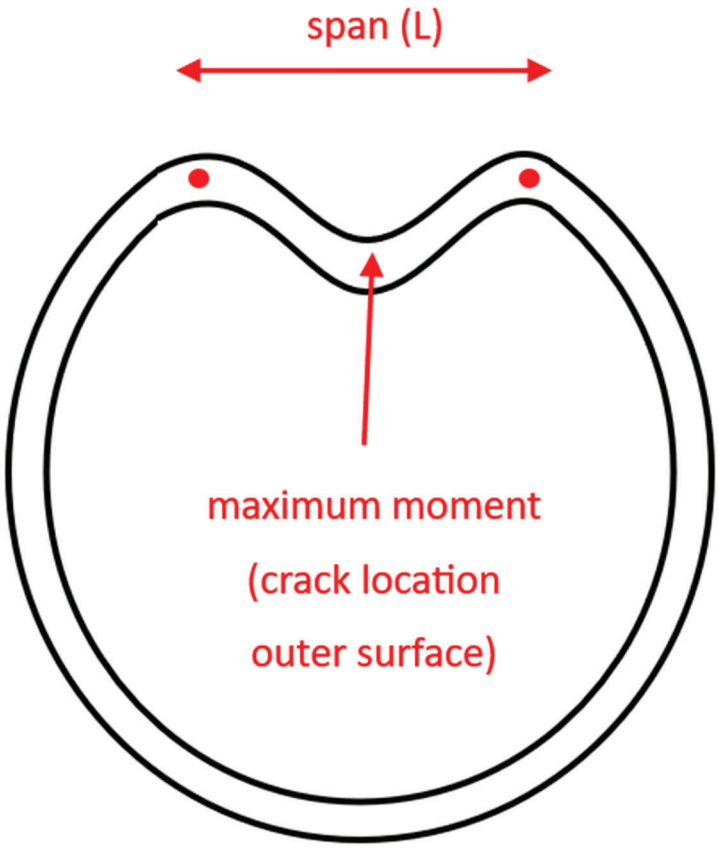

Figure 3 Schematic of unrestrained topside dent and simple beam analysis.

https://doi.org/10.52202/078572-0014

A standard approach to considering an "unrestrained" dent might use the former equation, with the freely supported span and n = 8. However, this is likely unrealistic, as the dent shoulders cannot be considered as zero-moment locations on the dent span. Another approach is to use the fixed span and n = 24, as the dent shoulders do impose restraint on the dent movement and moment in the pipe wall. The observation of cracking in the centre of this span suggests the ends of the span, the dent shoulders, are constrained to less than n = 12. The true conditions will be somewhere in between the two extremes. Note that the extremes vary by three times the moment.

Considering the cyclic moment in the centre of the span.

$$\Delta M \approx \frac{\Delta P}{24} \cdot L^2 = 90 \cdot \left(\frac{2 \cdot t_{nom}}{D}\right) \cdot \frac{2 \cdot D \cdot d}{24} = 15 \cdot t_{nom} \cdot d$$

Consider the bending stress in the centre of the span.

$$\Delta\sigma_{bend} = \Delta M \cdot \frac{c}{I} = 15 \cdot t_{nom} \cdot d \cdot \frac{6}{{t_{loc}}^2} = 90 \cdot \frac{t_{nom} \cdot d}{{t_{loc}}^2}$$

Note that the local thickness at the dent is used, where the pipe wall is flexing.

The total cyclic stress becomes...

$$\Delta\sigma_{max} = \Delta\sigma_{mem} + \Delta\sigma_{bend} = 90 \cdot \left(\frac{t_{nom}}{t_{loc}}\right) + 90 \cdot t_{nom} \cdot d \cdot \left(\frac{1}{t_{loc}}\right)^2$$

If there is no corrosion near the dent the calculation simplifies. However, the bending term will contribute substantially as the corrosion depth increases. Note for most dents of interest that the nominal wall thickness and dent depth terms will allow the bending term to dominate the stress analysis. The membrane stress becomes of lesser importance and can likely be disregarded.

Consider the RESTRAINED dent, typically bottom-side see **Figure 4**. Cracking usually occurs on the inside surface, at the centre of the rock, where the curvature is highest and the indenting tensile stress is maintained. The ends of the span are illustrated with red dot "hinge points". Note that in this case only half of the full dent span is considered for the beam bending analysis and the ends of the span are considered n = 12.

Consider a restrained dent. In this case, we assume half the dent span and the moment at the end of the span...

$$\Delta M \approx \frac{\Delta P}{12} \cdot \left(\frac{L}{2}\right)^2 \approx 90 \cdot \left(\frac{2 \cdot t_{nom}}{D}\right) \cdot \frac{2 \cdot D \cdot d}{12 \cdot 4} = 7.5 \cdot t_{nom} \cdot d$$

and...

$$\Delta\sigma_{max} = \Delta\sigma_{mem} + \Delta\sigma_{bend} = 90 \cdot \left(\frac{t_{nom}}{t_{loc}}\right) + 45 \cdot t_{nom} \cdot d \cdot \left(\frac{1}{t_{loc}}\right)^2$$

https://doi.org/10.52202/078572-0014

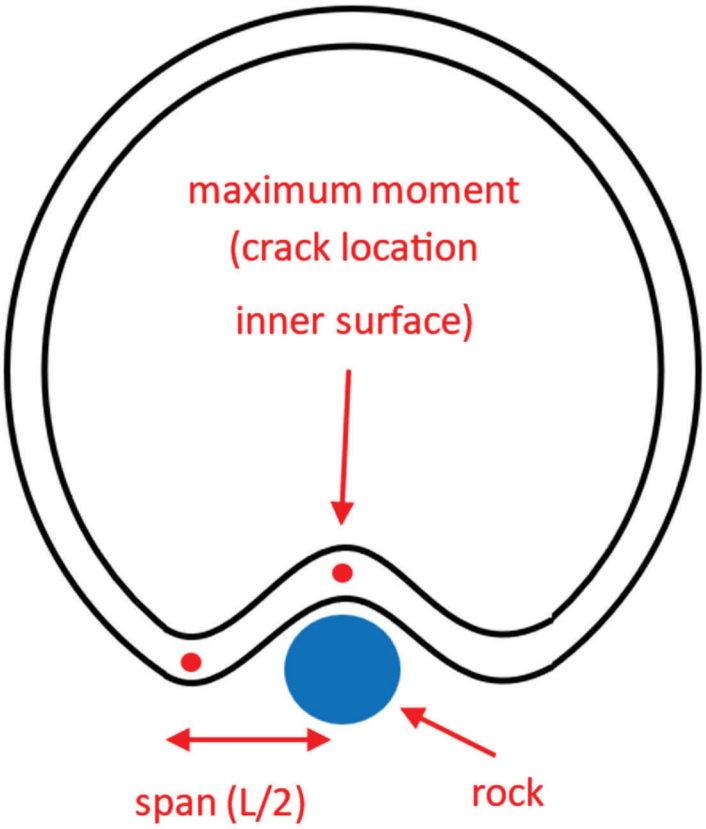

Figure 4 Schematic of restrained bottom-side dent and simple beam analysis.

In this case, the membrane stress is equal and the bending stress is HALF the value of the unrestrained dent. This becomes a very important relationship. With a Paris exponent of 3 assumed, we can expect a difference in fatigue life of (2^3 =) 8x between unrestrained and restrained dents. We also expect a dependence on the nominal wall thickness, dent depth, and localized wall thickness. The localized wall thickness term is squared, and so we expect a strong correlation in the data.

It is shown later that, for an unrestrained dent, the behavior of the simplified model is closer to the freely supported beam than the fixed end beam, with n = 10 at the center and n = 40 at the ends. For the restrained condition, the constraint factor "*n*" for all the data points is approximately 30 at the centre and 0 at the ends. Under these conditions, the ratio of unrestrained to restrained stress may increase to approximately 3.3.

2D / 3D Simplification

To evaluate our methodology for predicting the remaining life of indented pipes under pressure cycling, two numerical models were developed: a finite element Euler-Bernoulli (EB) beam model and a 2D finite element analysis (FEA) model for plane stress and plane strain conditions. These models provided insights into critical assumptions and uncertainties in our approach. They examined whether the straight beam in our simplified model behaves more like a simply supported or fixed-end beam. Additionally, they evaluated the impact of using plane stress instead of the plane strain and assessed how deep beam effects influence the validity of the Euler-Bernoulli assumption. To

https://doi.org/10.52202/078572-0014

maintain consistency, all models applied an internal pressure range corresponding to a 90 MPa hoop stress, calculated using Barlow's formula.

The EB beam model, implemented in Python, served as the primary tool. It represented half of the circumferential profile of the indented pipe as a series of EB beam elements (see **Figure 5**). Key parameters, including local and nominal wall thicknesses, dent depth, and outside diameter, were incorporated into this model. Mesh refinement was performed iteratively until the mechanical responses converged.

The 2D FEA models were constructed in Abaqus using Python scripting. These models also represented half of the circumferential profile but included the wall thickness dimension, and offering additional perspectives on the pipe's mechanical response. Material properties, including Young's modulus and Poisson's ratio, were applied. Boundary conditions were imposed at the top and bottom edges of the structure, adjusted based on the type of dent. The CPS4 element was used for the plane stress model, while the CPE4 element was used for the plane strain model. Mesh refinement was performed in each analysis to ensure accurate results (see **Figure 5**).

Table 1 compares the mechanical response of two extreme cases using EB and 2D FEA models, showing that the plane strain model produced slightly lower bending moments compared to the plane stress model at the dent location, while axial force differences between the two models were within 5%. Additionally, the plane stress model is closely aligned with the EB model results, particularly for the high (*OD/t*) ratio, supporting the use of the simplified EB approach.

Table 1 Mechanical responses for high and low (OD/t) ratios of an unrestrained dent, including axial force and bending moment at the indentation. Errors relative to the EB model are shown in parentheses.

OD (mm)	*t* (mm)	D (mm)	Model	N (kN)	M (kN.mm)
305	10	15	EB	0.861	5.35
			Plane Stress	0.832 (3.4%)	5.28 (1.3%)
			Plane Strain	0.832 (3.4%)	5.27 (1.5%)
910	8	45	EB	0.689	12.83
			Plane Stress	0.683 (0.9%)	12.77 (0.5%)
			Plane Strain	0.682 (1.0%)	12.68 (1.2%)

The EB model was applied to all data points to determine the constraint factors for the straight beam in the simplified model under both restrained and unrestrained conditions. For the unrestrained condition, the constraint factor "*n*" was approximately 10 at the centre and 40 at the ends, as shown in
Figure 6 (a). In contrast, for the restrained condition, the constraint factor "*n*" was approximately 30 at the centre and 0 at the ends, also illustrated in **Figure 6** (b). This analysis captures the variation in constraint factors between the two scenarios for all data points.

https://doi.org/10.52202/078572-0014

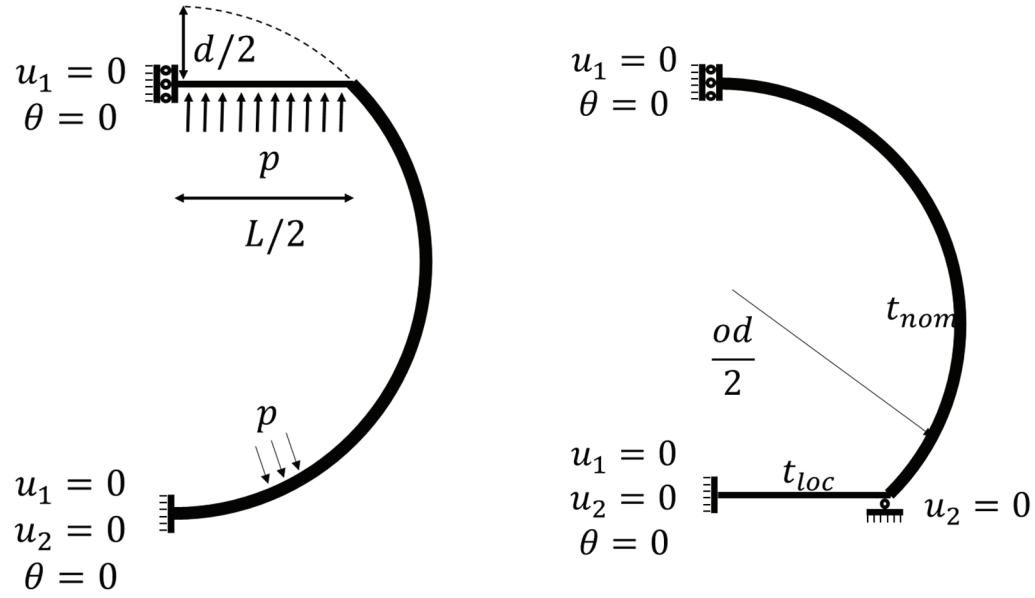

(a) Unrestrained condition (b) Restrained condition

Figure 5 Geometry, loading, and boundary conditions used for modelling the circumferential profile of a pressurized indented pipe.

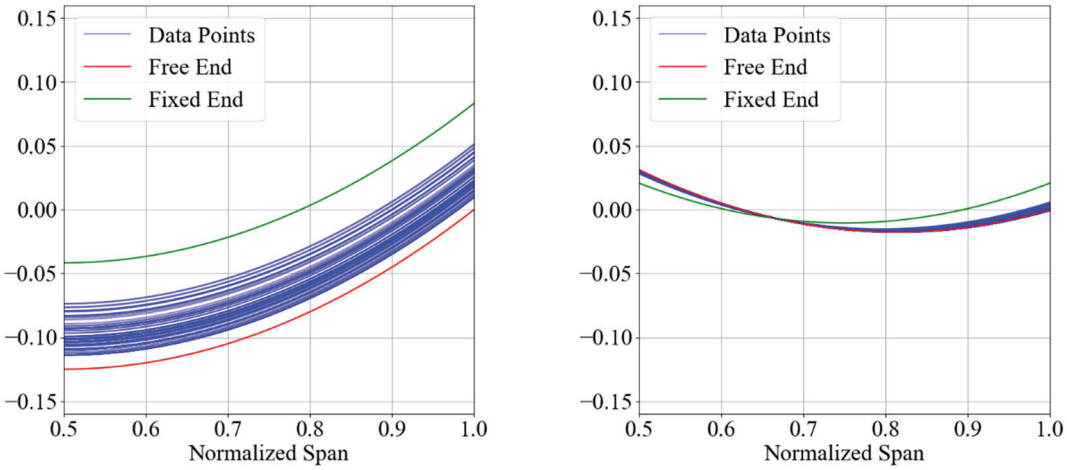

(a) Unrestrained (b) Restrained

Figure 6 Moment distribution along the simplified straight beam for all data points under restrained and unrestrained conditions, compared with the extreme cases where the ends (shoulders) are either fixed or free.

https://doi.org/10.52202/078572-0014

Model Development

The laboratory data was compiled. Each of the input parameters was plotted against the equivalent 90 MPa cycles to failure on a log-log plot. The unrestrained and restrained dents were isolated for comparison. Power law trend lines were applied, and the default statistics were reviewed for significance. Power law exponents close to 1/3 and 1/6 were expected, given the theoretical implications. In some cases, input parameters expected to show trends showed no correlations, indicating a less important consideration in the later modelling efforts. The effort was somewhat hindered by the unavoidably limited range of parameters in the test matrices.

The correlation that showed the most potential during the data analysis was the apparent relationship between the local wall thickness and the equivalent cycles to failure. **Figure 7** is a plot of this relationship for the test cases with corroded dents. These data were isolated, as they showed a clearer range of local thickness values. When all data are pooled, the relationship is obscured.

The data show two features of interest to this study. First; the trendlines applied to the data indicate a slope of near to (1/6). This value is consistent with an expected squared relationship between stress and local wall thickness, and a Paris law exponent of m = 3. Second; the difference between the remaining lives of the unrestrained and restrained data sets is approximately 8x, consistent with the two times differences in stress inferred from the beam constraint assumptions. This provided some confidence in the intended methodology.

This relationship was the one with the highest R^2 regression coefficient, and any indication of a theoretical basis. In other cases, there were no correlations. This is presumed due to either the limited range in the data, or the relationship observed was a compounded variable that could be reasonably attributed to the effect of the local wall thickness. The mathematics presented above suggest an influence of both nominal wall thickness and dent (absolute) depth, but this could not be confirmed by the data analysis. The local wall thickness parameter appears to dominate the fatigue life calculation. Again, this is a work in progress, and further data may clarify or refute this observation.

https://doi.org/10.52202/078572-0014

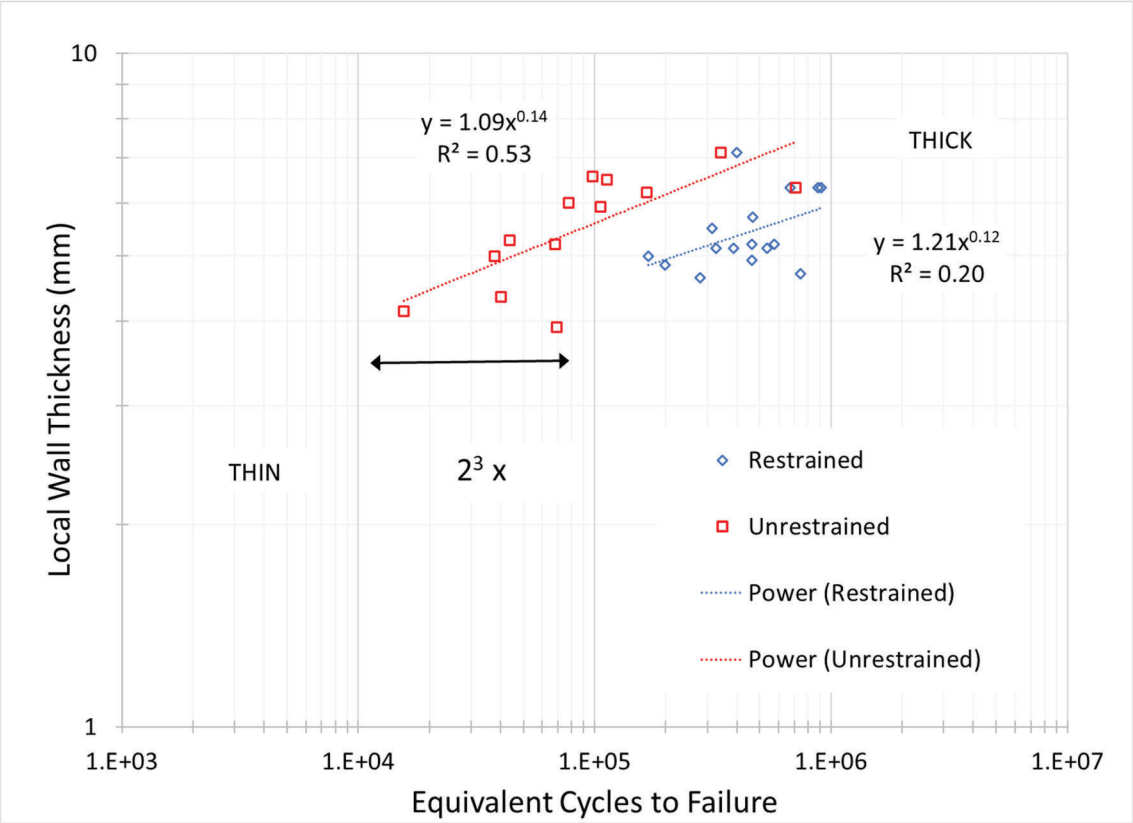

Figure 7 Plot of local wall thickness as a function of equivalent fatigue cycles to failure, for corroded dents data.

A simplified dent fatigue life model in the following form is proposed:

$$N_f = Constant \times \left(\frac{RF}{{t_{loc}}^2}\right)^3$$

where

Nf predicted equivalent fatigue cycles to failure
RF restraint factor, unrestrained = 1, restrained = 2

This equation provides a simplified model for screening of dents. It captures the key components of dent assessment of (1) a restraint factor to account for fatigue conditions acting on the dent and restricting or allowing flexibility, (2) the local wall thickness, which governs the cyclic stress acting on the dent due to in-service pressure fluctuations, (3) the squared exponent is consistent with beam theory, and (4) the cubed exponent is consistent with Paris Law. A restraint factor of 3.3 was also considered, based on the results of the FEA work, but model agreement was compromised.

Figure 8 is a plot of the equivalent cycles to failure for the complete data set, both model prediction and true laboratory measure values. This model relies largely on the consistency and correct set up of the laboratory by the test contractors. It presumes the test set-up is comparable to in-service conditions.

https://doi.org/10.52202/078572-0014

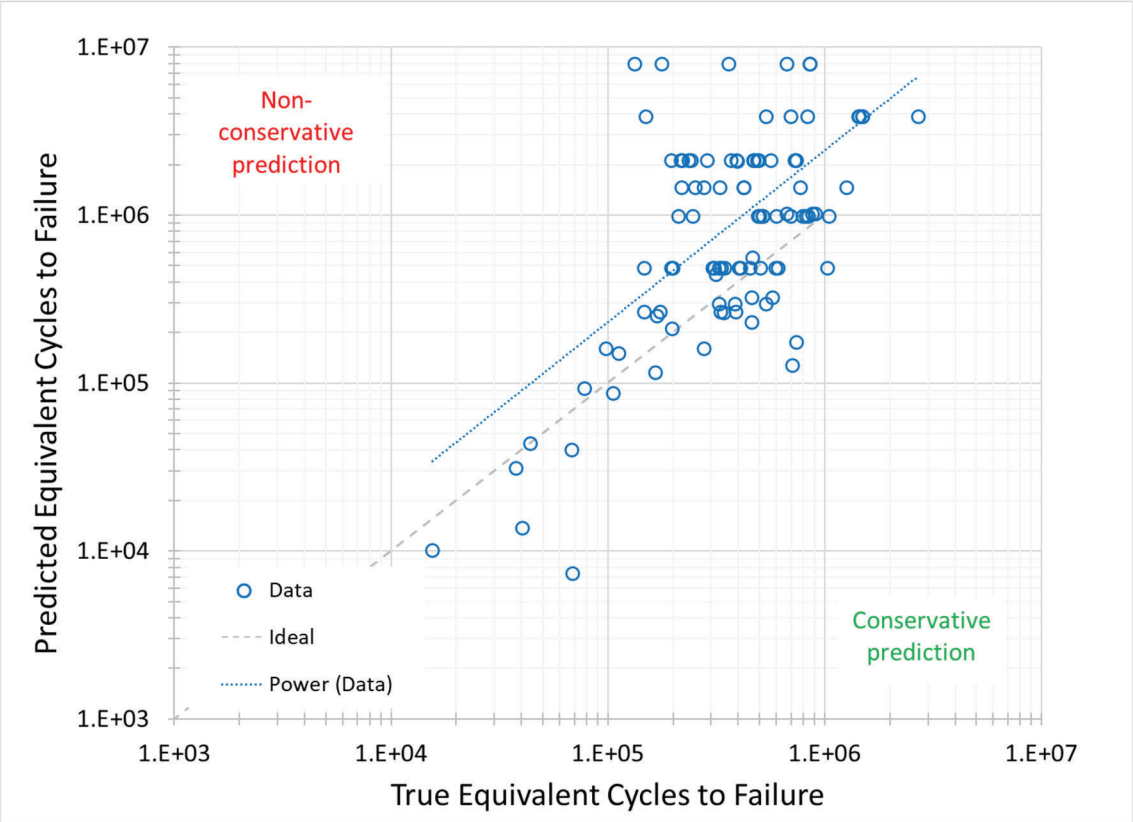

Figure 8 Plot of equivalent cycles to failure, prediction versus true values model comparison.

The constant is determined by regression and manually adjusted for effectiveness and efficiency. It will include fatigue S-N curve-type behaviour, although not explicitly. Analysts have the opportunity to adjust the constant for either accuracy or conservatism. The plot above indicates a model derived with conservatism in mind, the trend line through the actual data points is off the unity line, and dents with shorter remaining lives remain accurate or conservative.

Detractors of this methodology will highlight the data points above the unity and trendlines. This is a valid argument; the model is NOT conservative under all conditions. However, the data points that are non-conservative show remaining lives over 100,000 equivalent cycles to failure. Typically cycling of liquids pipelines is in the order of 100 - 200 equivalent cycles per year, so this issue only affects dents with predicted fatigue lives of 500 - 1,000 years. Analysts should be aware of this limitation. It should also be noted that this applies primarily to restrained dents, all of which demonstrated these high fatigue lives.

Detractors may also dispute an approach which does not explicitly consider "restraint", but infers that these situations represent dents with half the length of flexible span. For the "unrestrained" dents, the width between shoulders is used as the span, and the stress is evaluated at the centre of the span. For the "restrained" dents, the width between one shoulder and rock is used as the span, and the stress is evaluated at the end of the span. But both cases assume restraint at the ends of the

https://doi.org/10.52202/078572-0014

applicable span. This concept may be unverifiable, but it does appear to be supported by the available data and review of beam bending theory.

The model presented here is noticeably simplistic as compared to other available models. It does not delve into the details of the local strain at the dent apex. The data available in the industry literature does not seem to justify a focus in this area. The model also does not explicitly include dent depth, which one would expect to play a role. Other researchers have also noted a lack of a strong relationship to depth, though this is a point of discussion within industry.

Conclusions

This work has presented a simplified methodology for remaining life prediction of dents that may be considered as a screening tool for preliminary analysis. It is not considered definitive. Further industry data may reinforce or refute the relationships described. It is hoped that this work provides an alternative philosophy that other researchers may consider for ongoing studies. Consideration of dent "restraint" may be alternately viewed as dent "flexible span". In addition, the industry data suggests the local wall thickness is a primary contributor to fatigue life, and perhaps more attention should be put to this input parameter.

References

1. API 1183, *Assessment and Management of Pipeline Dents*, API Recommended Practice 1183, November 2020.
2. Leis (2024), *Commentary on API RP 1183 – Dent Assessment and Management*, B. N. Leis and A. Eshraghi, PPIM February 2024.
3. PHMSA (2012), *Dent Fatigue Life Assessment Close Out Report*, BMT Canada for DOT PHMSA #432 2012.
4. INGAA (2016), *Fatigue Considerations for Natural Gas Transmission Pipelines*, V. Semiga and A. Dinovitzer, (BMT Canada), INGAA reference 30348 FR Rev 02, June 2016.
5. PHMSA (2017), *Full Scale Testing of Interactive Features for Improved Models*, BMT and Engie R&I, US DOT PHMSA DTPH56-14-H-0002, September 2017.
6. PRCI (2018), *Full Scale Fatigue Testing of Dents (Plain Dents and Dents Interacting with Welds and Metal Loss*", PR-214-073510, 2018.
7. PRCI (2019), *Full Scale Testing of Shallow Dents with and without Interacting Features*, S. Tiku, A. Eshraghi, B. John and A. Dinovitzer (BMT Canada), PRCI Project MD-4-14, PR-214-163714-R01, October 2019.
8. PRCI (2022), *Improve Dent / Cracking Assessment Methods*, A. Rana, S. Tiku and A. Dinovitzer (BMT Canada), PRCI Project MD-5-2, PR-214-203806-R01, May 2022.
9. ASME B31.8 (2016), *Gas Transmission and Distribution Piping Systems*, ASME B31.8-2016.
10. ASME FFS-1 / API 579, "Fitness-for-Service", June 2016.
11. British Standard Institution 7910, "Guide to Methods for Assessing the Acceptability of Flaws in Metallic Structures", London, UK, 2013.
12. Cement Association of Canada, "*Concrete Design Handbook, 4th Edition*", 2017.

https://doi.org/10.52202/078572-0014